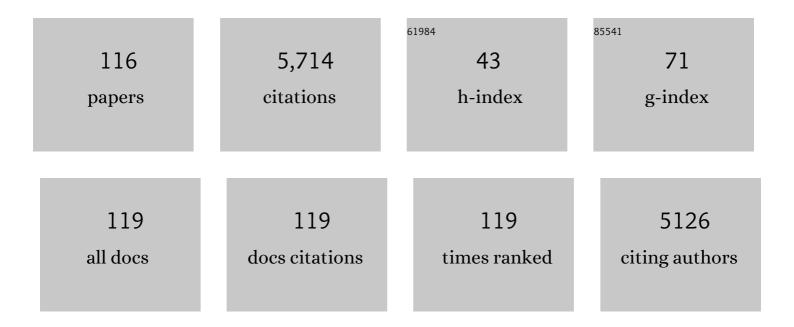
Christine V Putnis

List of Publications by Year in descending order

Source: https://exaly.com/author-pdf/6259207/publications.pdf Version: 2024-02-01



| # | Article | IF | CITATIONS |
|----|---------------------------------------------------------------------------------------------------------------------------------------------------------------------------------------------------------------------------------|------|-----------|
| 1 | The mechanism of reequilibration of solids in the presence of a fluid phase. Journal of Solid State Chemistry, 2007, 180, 1783-1786. | 2.9 | 328 |
| 2 | The dissolution rates of natural glasses as a function of their composition at pH 4 and 10.6, and temperatures from 25 to 74°C. Geochimica Et Cosmochimica Acta, 2004, 68, 4843-4858. | 3.9 | 321 |
| 3 | Coupled dissolution and precipitation at mineral–fluid interfaces. Chemical Geology, 2014, 383, 132-146. | 3.3 | 290 |
| 4 | Direct observations of pseudomorphism: compositional and textural evolution at a fluid-solid interface. American Mineralogist, 2005, 90, 1909-1912. | 1.9 | 183 |
| 5 | Direct observation of heavy metal-mineral association from the Clark Fork River Superfund Complex: Implications for metal transport and bioavailability. Geochimica Et Cosmochimica Acta, 2005, 69, 1651-1663. | 3.9 | 169 |
| 6 | Reaction induced fracturing during replacement processes. Contributions To Mineralogy and Petrology, 2009, 157, 127-133. | 3.1 | 163 |
| 7 | The role of background electrolytes on the kinetics and mechanism of calcite dissolution. Geochimica Et Cosmochimica Acta, 2010, 74, 1256-1267. | 3.9 | 128 |
| 8 | Mechanism of leached layer formation during chemical weathering of silicate minerals. Geology, 2012, 40, 947-950. | 4.4 | 127 |
| 9 | The Mineral-Water Interface: Where Minerals React with the Environment. Elements, 2013, 9, 177-182. | 0.5 | 116 |
| 10 | Hematite in porous red-clouded feldspars: Evidence of large-scale crustal fluid–rock interaction. Lithos, 2007, 95, 10-18. | 1.4 | 114 |
| 11 | Direct observations of mineral fluid reactions using atomic force microscopy: the specific example of calcite. Mineralogical Magazine, 2012, 76, 227-253. | 1.4 | 109 |
| 12 | The effect of cation:anion ratio in solution on the mechanism of barite growth at constant supersaturation: Role of the desolvation process on the growth kinetics. Geochimica Et Cosmochimica Acta, 2007, 71, 5168-5179. | 3.9 | 105 |
| 13 | Dissolution and Carbonation of Portlandite [Ca(OH) ₂] Single Crystals. Environmental Science & Technology, 2013, 47, 11342-11349. | 10.0 | 105 |
| 14 | An experimental study of the replacement of leucite by analcime. American Mineralogist, 2007, 92, 19-26. | 1.9 | 104 |
| 15 | Environmentally important, poorly crystalline Fe/Mn hydrous oxides: Ferrihydrite and a possibly new vernadite-like mineral from the Clark Fork River Superfund Complex. American Mineralogist, 2005, 90, 718-724. | 1.9 | 101 |
| 16 | A mechanism of mineral replacement: isotope tracing in the model system KCl-KBr-H2O. Geochimica Et Cosmochimica Acta, 2004, 68, 2839-2848. | 3.9 | 99 |
| 17 | An atomic force microscopy study of calcite dissolution in saline solutions: The role of magnesium ions. Geochimica Et Cosmochimica Acta, 2009, 73, 3201-3217. | 3.9 | 99 |
| 18 | Direct Nanoscale Observations of CO ₂ Sequestration during Brucite [Mg(OH) ₂] Dissolution. Environmental Science & Technology, 2012, 46, 5253-5260. | 10.0 | 97 |

| # | Article | IF | CITATIONS |
|----|---------------------------------------------------------------------------------------------------------------------------------------------------------------------------------------------------------------------|------|-----------|
| 19 | Kinetics of Calcium Phosphate Nucleation and Growth on Calcite: Implications for Predicting the Fate of Dissolved Phosphate Species in Alkaline Soils. Environmental Science & Technology, 2012, 46, 834-842. | 10.0 | 92 |
| 20 | Direct Nanoscale Imaging Reveals the Growth of Calcite Crystals via Amorphous Nanoparticles. Crystal Growth and Design, 2016, 16, 1850-1860. | 3.0 | 89 |
| 21 | The mechanism of cation and oxygen isotope exchange in alkali feldspars under hydrothermal conditions. Contributions To Mineralogy and Petrology, 2009, 157, 65-76. | 3.1 | 86 |
| 22 | Effect of pH on calcite growth at constant ratio and supersaturation. Geochimica Et Cosmochimica Acta, 2011, 75, 284-296. | 3.9 | 84 |
| 23 | Mineral replacement reactions in solid solution-aqueous solution systems: Volume changes, reactions paths and end-points using the example of model salt systems. Numerische Mathematik, 2011, 311, 211-236. | 1.4 | 72 |
| 24 | Posner's cluster revisited: direct imaging of nucleation and growth of nanoscale calcium phosphate clusters at the calcite-water interface. CrystEngComm, 2012, 14, 6252. | 2.6 | 71 |
| 25 | Control of silicate weathering by interface-coupled dissolution-precipitation processes at the mineral-solution interface. Geology, 2016, 44, 567-570. | 4.4 | 68 |
| 26 | In Situ Nanoscale Imaging of Struvite Formation during the Dissolution of Natural Brucite: Implications for Phosphorus Recovery from Wastewaters. Environmental Science & Technology, 2016, 50, 13032-13041. | 10.0 | 65 |
| 27 | Ion-specific effects on the kinetics of mineral dissolution. Chemical Geology, 2011, 281, 364-371. | 3.3 | 64 |
| 28 | Textural Evolution of Plagioclase Feldspar across a Shear Zone: Implications for Deformation Mechanism and Rock Strength. Journal of Petrology, 2014, 55, 1457-1477. | 2.8 | 62 |
| 29 | The mechanism and kinetics of DTPA-promoted dissolution of barite. Applied Geochemistry, 2008, 23, 2778-2788. | 3.0 | 60 |
| 30 | Interactions of arsenic with calcite surfaces revealed by in situ nanoscale imaging. Geochimica Et Cosmochimica Acta, 2015, 159, 61-79. | 3.9 | 60 |
| 31 | Specific effects of background electrolytes on the kinetics of step propagation during calcite growth. Geochimica Et Cosmochimica Acta, 2011, 75, 3803-3814. | 3.9 | 57 |
| 32 | Selenium incorporation into calcite and its effect on crystal growth: An atomic force microscopy study. Chemical Geology, 2013, 340, 151-161. | 3.3 | 57 |
| 33 | An Atomic Force Microscopy study of the growth of calcite in the presence of sodium sulfate. Chemical Geology, 2008, 253, 243-251. | 3.3 | 56 |
| 34 | In situ Imaging of Interfacial Precipitation of Phosphate on Goethite. Environmental Science & Technology, 2015, 49, 4184-4192. | 10.0 | 56 |
| 35 | Modelling the effects of salt solutions on the hydration of calcium ions. Physical Chemistry Chemical Physics, 2014, 16, 7772-7785. | 2.8 | 54 |
| 36 | The experimental replacement of ilmenite by rutile in HCl solutions. Mineralogical Magazine, 2010, 74, 633-644. | 1.4 | 53 |

| # | Article | IF | CITATIONS |
|----|--------------------------------------------------------------------------------------------------------------------------------------------------------------------------------------------------------------------------------|------|-----------|
| 37 | In situ nanoscale observations of the dissolution of dolomite cleavage surfaces. Geochimica Et Cosmochimica Acta, 2012, 80, 1-13. | 3.9 | 53 |
| 38 | An Atomic Force Microscopy Study of the Growth of a Calcite Surface as a Function of Calcium/Total Carbonate Concentration Ratio in Solution at Constant Supersaturation. Crystal Growth and Design, 2009, 9, 4344-4350. | 3.0 | 52 |
| 39 | An atomic force microscopy and molecular simulations study of the inhibition of barite growth by phosphonates. Surface Science, 2004, 553, 61-74. | 1.9 | 48 |
| 40 | Zircon coronas around Fe–Ti oxides: a physical reference frame for metamorphic and metasomatic reactions. Contributions To Mineralogy and Petrology, 2008, 156, 517-527. | 3.1 | 48 |
| 41 | The influence of pH on barite nucleation and growth. Chemical Geology, 2015, 391, 7-18. | 3.3 | 48 |
| 42 | Crystal growth of apatite by replacement of an aragonite precursor. Journal of Crystal Growth, 2010, 312, 2431-2440. | 1.5 | 47 |
| 43 | Molecular Understanding of Humic Acid-Limited Phosphate Precipitation and Transformation. Environmental Science & Technology, 2020, 54, 207-215. | 10.0 | 46 |
| 44 | In situ AFM study of the dissolution and recrystallization behaviour of polished and stressed calcite surfaces. Geochimica Et Cosmochimica Acta, 2006, 70, 1728-1738. | 3.9 | 44 |
| 45 | Mechanistic Principles of Barite Formation: From Nanoparticles to Micron-Sized Crystals. Crystal Growth and Design, 2015, 15, 3724-3733. | 3.0 | 43 |
| 46 | Direct Observation of Spiral Growth, Particle Attachment, and Morphology Evolution of Hydroxyapatite. Crystal Growth and Design, 2016, 16, 4509-4518. | 3.0 | 43 |
| 47 | Pseudomorphic replacement of single calcium carbonate crystals by polycrystalline apatite. Mineralogical Magazine, 2008, 72, 77-80. | 1.4 | 42 |
| 48 | An atomic force microscopy study of the dissolution of calcite in the presence of phosphate ions. Geochimica Et Cosmochimica Acta, 2013, 117, 115-128. | 3.9 | 42 |
| 49 | Peridotite weathering is the missing ingredient of Earth's continental crust composition. Nature Communications, 2018, 9, 634. | 12.8 | 36 |
| 50 | Direct Observations of the Occlusion of Soil Organic Matter within Calcite. Environmental Science & Technology, 2019, 53, 8097-8104. | 10.0 | 35 |
| 51 | Timescales of interface-coupled dissolution-precipitation reactions on carbonates. Geoscience Frontiers, 2019, 10, 17-27. | 8.4 | 34 |
| 52 | The mechanism of fluid infiltration in peridotites at Almklovdalen, western Norway. Geofluids, 2002, 2, 203-215. | 0.7 | 33 |
| 53 | Dissolution and Precipitation Dynamics at Environmental Mineral Interfaces Imaged by In Situ Atomic Force Microscopy. Accounts of Chemical Research, 2020, 53, 1196-1205. | 15.6 | 33 |
| 54 | Crystal Growth and Dissolution of Calcite in the Presence of Fluoride Ions: An Atomic Force Microscopy Study. Crystal Growth and Design, 2010, 10, 60-69. | 3.0 | 30 |

| # | Article | IF | CITATIONS |
|----|------------------------------------------------------------------------------------------------------------------------------------------------------------------------------------------------------------------------|------------------|-----------|
| 55 | Direct nanoscale observations of the coupled dissolution of calcite and dolomite and the precipitation of gypsum. Beilstein Journal of Nanotechnology, 2014, 5, 1245-1253. | 2.8 | 30 |
| 56 | Experimental study of the replacement of calcite by calcium sulphates. Geochimica Et Cosmochimica Acta, 2015, 156, 75-93. | 3.9 | 30 |
| 57 | Coupled Dissolution and Precipitation at the Cerussite-Phosphate Solution Interface: Implications for Immobilization of Lead in Soils. Environmental Science & Technology, 2013, 47, 13502-13510. | 10.0 | 29 |
| 58 | Sequestration of Selenium on Calcite Surfaces Revealed by Nanoscale Imaging. Environmental Science & Technology, 2013, 47, 13469-13476. | 10.0 | 28 |
| 59 | Interactions between mineral surfaces and dissolved species: From monovalent ions to complex organic molecules. Numerische Mathematik, 2005, 305, 791-825. | 1.4 | 27 |
| 60 | The pseudomorphic replacement of marble by apatite: The role of fluid composition. Chemical Geology, 2016, 425, 1-11. | 3.3 | 27 |
| 61 | Siderite dissolution coupled to iron oxyhydroxide precipitation in the presence of arsenic revealed by nanoscale imaging. Chemical Geology, 2017, 449, 123-134. | 3.3 | 27 |
| 62 | The effect of fluid composition on the mechanism of the aragonite to calcite transition. Mineralogical Magazine, 2008, 72, 111-114. | 1.4 | 26 |
| 63 | Hydration Effects on the Stability of Calcium Carbonate Pre-Nucleation Species. Minerals (Basel,) Tj ETQq1 1 0.78 | 4314 rgBT 2.0 | /Overlock |
| 64 | Molecular-Scale Investigations Reveal Noncovalent Bonding Underlying the Adsorption of Environmental DNA on Mica. Environmental Science & Technology, 2019, 53, 11251-11259. | 10.0 | 26 |
| 65 | Interactions between Organophosphonate-Bearing Solutions and (101Ì4) Calcite Surfaces: An Atomic Force Microscopy and First-Principles Molecular Dynamics Study. Crystal Growth and Design, 2010, 10, 3022-3035. | 3.0 | 25 |
| 66 | The replacement of a carbonate rock by fluorite: Kinetics and microstructure. American Mineralogist, 2017, 102, 126-134. | 1.9 | 25 |
| 67 | Interfacial Precipitation of Phosphate on Hematite and Goethite. Minerals (Basel, Switzerland), 2018, 8, 207. | 2.0 | 25 |
| 68 | Humic Acids Limit the Precipitation of Cadmium and Arsenate at the Brushite–Fluid Interface. Environmental Science & Technology, 2019, 53, 194-202. | 10.0 | 25 |
| 69 | Exploring the effect of poly(acrylic acid) on pre- and post-nucleation BaSO ₄ species: new insights into the mechanisms of crystallization control by polyelectrolytes. CrystEngComm, 2016, 18, 2830-2842. | 2.6 | 24 |
| 70 | Interaction between Epsomite Crystals and Organic Additives. Crystal Growth and Design, 2008, 8, 2665-2673. | 3.0 | 23 |
| 71 | Hydration effects on gypsum dissolution revealed by in situ nanoscale atomic force microscopy observations. Geochimica Et Cosmochimica Acta, 2016, 179, 110-122. | 3.9 | 23 |
| 72 | Sequestration of Antimony on Calcite Observed by Time-Resolved Nanoscale Imaging. Environmental Science & Technology, 2018, 52, 107-113. | 10.0 | 23 |

| # | Article | IF | CITATIONS |
|----|---------------------------------------------------------------------------------------------------------------------------------------------------------------------------------------|------|-----------|
| 73 | Underlying Role of Brushite in Pathological Mineralization of Hydroxyapatite. Journal of Physical Chemistry B, 2019, 123, 2874-2881. | 2.6 | 23 |
| 74 | Influence of chemical and structural factors on the calcite–calcium oxalate transformation. CrystEngComm, 2013, 15, 9968. | 2.6 | 22 |
| 75 | Coupled fluctuations in element release during dolomite dissolution. Mineralogical Magazine, 2014, 78, 1355-1362. | 1.4 | 22 |
| 76 | Imaging Organophosphate and Pyrophosphate Sequestration on Brucite by in Situ Atomic Force Microscopy. Environmental Science & Technology, 2017, 51, 328-336. | 10.0 | 21 |
| 77 | Direct Observation of Simultaneous Immobilization of Cadmium and Arsenate at the Brushite–Fluid Interface. Environmental Science & Technology, 2018, 52, 3493-3502. | 10.0 | 21 |
| 78 | Metal Sequestration through Coupled Dissolution–Precipitation at the Brucite–Water Interface. Minerals (Basel, Switzerland), 2018, 8, 346. | 2.0 | 21 |
| 79 | Base-metals and organic content in stream sediments in the vicinity of a landfill. Applied Geochemistry, 2004, 19, 137-151. | 3.0 | 20 |
| 80 | Direct observations of the modification of calcite growth morphology by Li+ through selectively stabilizing an energetically unfavourable face. CrystEngComm, 2011, 13, 3962. | 2.6 | 20 |
| 81 | Mechanisms of Modulation of Calcium Phosphate Pathological Mineralization by Mobile and Immobile Small-Molecule Inhibitors. Journal of Physical Chemistry B, 2018, 122, 1580-1587. | 2.6 | 20 |
| 82 | AFM study of the epitaxial growth of brushite (CaHPO4{middle dot}2H2O) on gypsum cleavage surfaces. American Mineralogist, 2010, 95, 1747-1757. | 1.9 | 19 |
| 83 | Effect of ferrous iron on the nucleation and growth of CaCO ₃ in slightly basic aqueous solutions. CrystEngComm, 2017, 19, 447-460. | 2.6 | 19 |
| 84 | Removal of Fe(II) from groundwater via aqueous portlandite carbonation and calcite-solution interactions. Chemical Engineering Journal, 2016, 283, 404-411. | 12.7 | 17 |
| 85 | Template-Assisted Crystallization of Sulfates onto Calcite: Implications for the Prevention of Salt Damage. Crystal Growth and Design, 2013, 13, 40-51. | 3.0 | 16 |
| 86 | Visualizing Organophosphate Precipitation at the Calcite–Water Interface by in Situ Atomic-Force Microscopy. Environmental Science & Technology, 2016, 50, 259-268. | 10.0 | 15 |
| 87 | Direct imaging of coupled dissolution-precipitation and growth processes on calcite exposed to chromium-rich fluids. Chemical Geology, 2020, 552, 119770. | 3.3 | 15 |
| 88 | The Control of Solution Composition on Ligand-Promoted Dissolution: DTPAâ^'Barite Interactions. Crystal Growth and Design, 2009, 9, 5266-5272. | 3.0 | 14 |
| 89 | Direct Observations of the Dissolution of Fluorite Surfaces with Different Orientations. Crystal Growth and Design, 2014, 14, 69-77. | 3.0 | 14 |
| 90 | Porosity generated during the fluid-mediated replacement of calcite by fluorite. CrystEngComm, 2016, 18, 6867-6874. | 2.6 | 14 |

| # | Article | IF | CITATIONS |
|-----|------------------------------------------------------------------------------------------------------------------------------------------------------------------------------------|------|-----------|
| 91 | In Situ Atomic Force Microscopy Imaging of Octacalcium Phosphate Crystallization and Its Modulation by Amelogenin's C-Terminus. Crystal Growth and Design, 2017, 17, 2194-2202. | 3.0 | 14 |
| 92 | Influence of pH and citrate on the formation of oxalate layers on calcite revealed by in situ nanoscale imaging. CrystEngComm, 2017, 19, 3420-3429. | 2.6 | 14 |
| 93 | Direct observations of the influence of solution composition on magnesite dissolution. Geochimica Et Cosmochimica Acta, 2013, 109, 113-126. | 3.9 | 13 |
| 94 | Nanoparticles formed during mineral-fluid interactions. Chemical Geology, 2021, 586, 120614. | 3.3 | 13 |
| 95 | Phosphorylated/Nonphosphorylated Motifs in Amelotin Turn Off/On the Acidic Amorphous Calcium Phosphate-to-Apatite Phase Transformation. Langmuir, 2020, 36, 2102-2109. | 3.5 | 12 |
| 96 | Energetic Basis for Inhibition of Calcium Phosphate Biomineralization by Osteopontin. Journal of Physical Chemistry B, 2017, 121, 5968-5976. | 2.6 | 11 |
| 97 | Nanoscale imaging of the simultaneous occlusion of nanoplastics and glyphosate within soil minerals. Environmental Science: Nano, 2021, 8, 2855-2865. | 4.3 | 11 |
| 98 | Atomic force microscopy imaging of classical and nonclassical surface growth dynamics of calcium orthophosphates. CrystEngComm, 2018, 20, 2886-2896. | 2.6 | 10 |
| 99 | The effect of a copolymer inhibitor on baryte precipitation. Mineralogical Magazine, 2014, 78, 1423-1430. | 1.4 | 9 |
| 100 | Dynamics and Molecular Mechanism of Phosphate Binding to a Biomimetic Hexapeptide. Environmental Science & Technology, 2018, 52, 10472-10479. | 10.0 | 9 |
| 101 | Dynamic force spectroscopy for quantifying single-molecule organo–mineral interactions. CrystEngComm, 2021, 23, 11-23. | 2.6 | 8 |
| 102 | Face-Specific Occlusion of Lipid Vesicles within Calcium Oxalate Monohydrate. Crystal Growth and Design, 2021, 21, 2398-2404. | 3.0 | 8 |
| 103 | Facet-Specific Dissolution–Precipitation at Struvite–Water Interfaces. Crystal Growth and Design, 2021, 21, 4111-4120. | 3.0 | 8 |
| 104 | A potentiometric study of the performance of a commercial copolymer in the precipitation of scale forming minerals. CrystEngComm, 2016, 18, 5744-5753. | 2.6 | 7 |
| 105 | Mineral Surface Rearrangement at High Temperatures: Implications for Extraterrestrial Mineral Grain Reactivity. ACS Earth and Space Chemistry, 2017, 1, 113-121. | 2.7 | 7 |
| 106 | Inhibition of Spiral Growth and Dissolution at the Brushite (010) Interface by Chondroitin 4-Sulfate. Journal of Physical Chemistry B, 2019, 123, 845-851. | 2.6 | 7 |
| 107 | Relative rates of fluid advection, elemental diffusion and replacement govern reaction front patterns. Earth and Planetary Science Letters, 2021, 565, 116950. | 4.4 | 7 |
| 108 | <i>In situ</i> observations of the occlusion of a clay-sugar compound within calcite. Environmental Science: Nano, 2022, 9, 523-531. | 4.3 | 6 |

| # | Article | IF | CITATIONS |
|-----|------------------------------------------------------------------------------------------------------------------------------------------------------------------------|-------------------|-------------|
| 109 | Baryte cohesive layers formed on a (010) gypsum surface by a pseudomorphic replacement. European Journal of Mineralogy, 2019, 31, 289-299. | 1.3 | 5 |
| 110 | Crystallization via Nonclassical Pathways: Nanoscale Imaging of Mineral Surfaces. ACS Symposium Series, 0, , 1-35. | 0.5 | 3 |
| 111 | Macro- to nanoscale study of the effect of aqueous sulphate on calcite growth. Mineralogical Magazine, 2008, 72, 141-144. | 1.4 | 2 |
| 112 | Halide-Dependent Dissolution of Dicalcium Phosphate Dihydrate and Its Modulation by an Organic Ligand. Crystal Growth and Design, 2017, 17, 3868-3876. | 3.0 | 2 |
| 113 | Direct Observations of the Coupling between Quartz Dissolution and Mg-Silicate Formation. ACS Earth and Space Chemistry, 2019, 3, 617-625. | 2.7 | 2 |
| 114 | Ion partitioning and element mobilization during mineral replacement reactions in natural and experimental systems. , 0, , 189-226. | | 2 |
| 115 | Editorial for Special Issue "Mineral Surface Reactions at the Nanoscale― Minerals (Basel,) Tj ETQq1 1 0.7843 | 814 rgBT / 2.0 | Overlock 10 |
| 116 | Mineral reactivity: from biomineralization and Earth's climate evolution, to CO2 capture and monument conservation. European Journal of Mineralogy, 2019, 31, 205-207. | 1.3 | 0 |